Structural Engineering and Mechanics, Vol. 3, No. 4 (1995) 299-312
DOI: http://dx.doi.org/10.12989/sem.1995.3.4.299

A new reinforcing steel model with bond-slip

H.G. Kwak†

Samsung Engineering and Construction Co., Kangnam P.O. Box 1430, Seoul 135-080, Korea

F.C. Filippou‡

Dept. of Civil Engineering, University of California at Berkeley, Berkeley, California 94720, U.S.A.

Abstract. A new reinforcing steel model which is embedded inside a concrete element and also accounts for the effect of bond-slip is developed. Unlike the classical bond-link or bond-zone element using double nodes, the proposed model is considering the bond-slip effect without taking double nodes by incorporation of the equivalent steel stiffness. After calculation of nodal displacements, the deformation of steel at each node can be found through the back-substitution technique from the first to the final steel element using a governing equation constructed based on the equilibrium at each node of steel and the compatibility condition between steel and concrete. This model results in significant savings in the number of nodes needed to account for the effect of bond-slip, in particular, when the model is used for three dimensional finite element problems. Moreover a new nonlinear solution scheme is developed in connection with this model. Finally, correlation studies between analytical and experimental results and several parameter studies are conducted with the objective to establish the validity of the proposed model.

Key words: bond-slip; steel model; double node; solution algorithm; equilibrium.

1. Introduction

Reinforced concrete(RC) structures are made up of two materials with different characteristics, namely, concrete and steel. Steel can be considered as a homogeneous material and its material properties are generally well defined. On the other hand, concrete is a heterogeneous material made up of cement, mortar and aggregates and exhibits nonlinear behavior even under low level loading due to nonlinear material behavior, environmental effects, cracking, biaxial stiffening and strain softening. Moreover, reinforcing steel and concrete interact in a complex way through bond-slip and aggregate interlock. These complex phenomena have led engineers in the past to rely heavily on empirical formulas for the design of concrete structures, which were derived from numerous experiments. With the advent of digital computers and powerful methods of analysis, such as the finite element method, many efforts to develop analytical solutions which would complement the experiments have been undertaken by investigators (Leibengood, *et al.* 1986, Choi and Kwak 1990). In spite of the large number of previous studies on the nonlinear finite element analysis of reinforced concrete structures, only few conclusions of general applicabi-

† Senior Researcher
‡ Professor

lity have been arrived at. The inclusion of the effects of tension stiffening and bond-slip is the case in point. Since few rational models of this difficult problem have been proposed so far, it is rather impossible to assess exactly what aspects of the behavior are included in each study and what the relative contribution of each is.

While the response of lightly reinforced beams in bending is very sensitive to the effect of tension stiffening of concrete, the response of RC structures in which shear plays an important role, such as over-reinforced beams and shear wall, is much more affected by the bond-slip of reinforcing steel than the tension stiffening of concrete (Kwak and Filippou 1990). To account for the bond-slip of reinforcing steel two different approaches are common in the finite element analysis of reinforced concrete structures. The first approach makes use of the bond-link element proposed by Ngo and Scordelis (1967). This element connects a node of a concrete finite element with a node of an adjacent steel element. The link element has no physical dimensions, i.e., the two connected nodes have the same coordinates(Fig. 1a). The second approach makes use of the bond-zone element developed by de Groot, *et al.* (1981). In this element the behavior of the contact surface between steel and concrete and the behavior of the concrete in the immediate vicinity of the reinforcing bar is described by a material law which considers the special properties of the bond zone. The contact element provides a continuous connection between reinforcing steel and concrete, if a linear or higher order displacement field is used in the discretization scheme(Fig. 1b). A simpler but similar element was proposed by Keuser and Mehlhorn (1987) who showed that the bond-link element cannot represent adequately the stiffness of the steel-concrete interface. Even though many studies of the bond-slip relationship between reinforcing steel and concrete have been conducted, considerable uncertainty about this complex phenomenon still exists because of the many parameters which are involved. Especially the complication in numerical modeling caused by taking the double nodes exacts that most finite element studies of RC structures do not account for bond-slip of reinforcing steel. Many researchers express the opinion that this effect is included in the tension stiffening model.

In this study, a new reinforcing steel model which is embedded inside a concrete element and accounts for the effect of bond-slip without taking the double nodes is developed. The reliability for the proposed model is verified through the correlation studies between analytical and experimental results.

2. Reinforcing steel model with bond-slip

2.1. General

Bond is the interaction between reinforcing steel and surrounding concrete. Since bond stresses in reinforced concrete members arise from the change in the steel force along the length, the effect of bond becomes more pronounced at the end anchorages of reinforcing bars and in the vicinity of cracks.

In the simplified analysis of reinforced concrete structures complete, compatibility of strains between concrete and steel is usually assumed, which implies perfect bond. This assumption is realistic only in regions where negligible stress transfer between the two components takes place. In the regions of transfer stresses along the interface between reinforcing steel and sur rounding concrete, especially near cracks, the bond stress is related to the relative displacement between reinforcing steel and concrete. The assumption of perfect bond near crack zones requires infinitely high strains to explain the existence of a finite crack width. In reality there is no

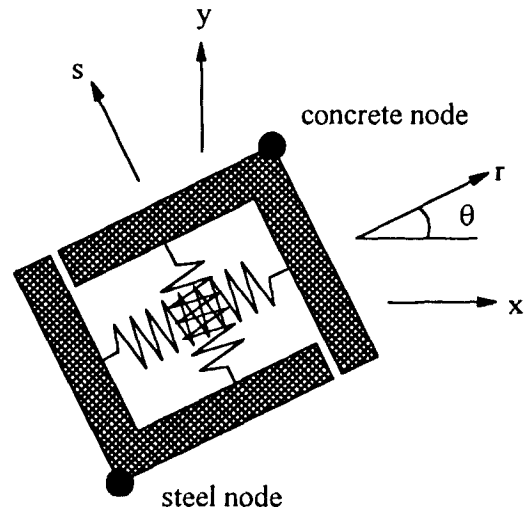

(a) Bond-Link Element

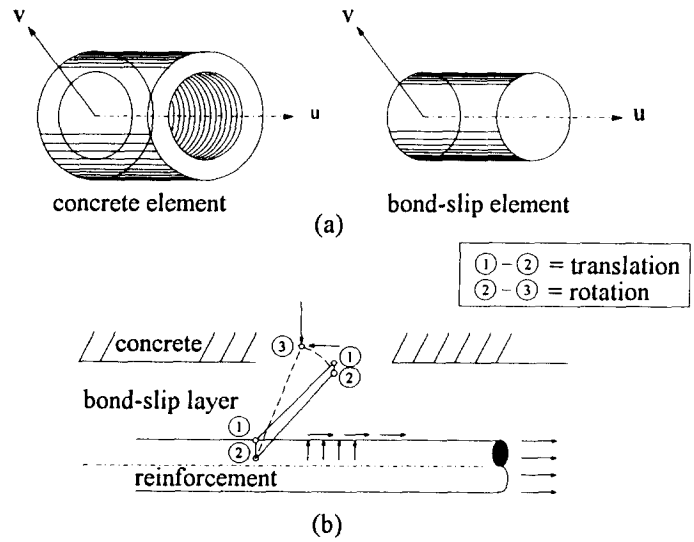

(b) Bond-Zone Element

Fig. 1 Bond models.

strain compatibility between reinforcing steel and surrounding concrete near cracks. This incompatibility and the crack propagation give rise to relative displacements between steel and concrete, which are known as the bond-slip.

Two basically different elements, namely, the bond-link element and bond-zone element, have been proposed to date for inclusion of the bond-slip effect in the finite element analysis of RC structures as mensioned above. In studies where the detailed local behavior is of interest, the continuous bond elements such as bond-zone elements are most appropriate. In cases, however, where the overall structural behavior is of primary interest, the bond-link element provides

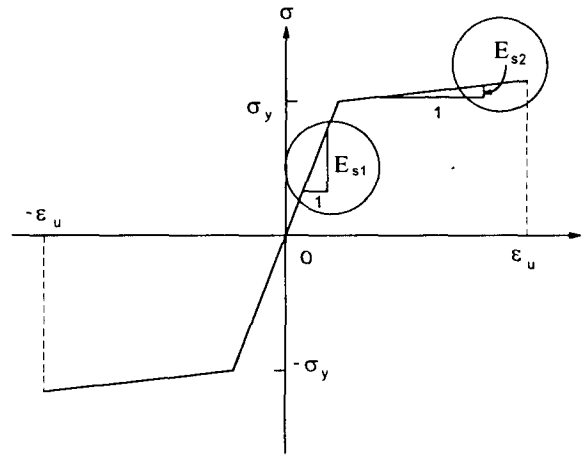

Fig. 2 Stress-strain relationship of steel.

a reasonable compromise between accuracy and computational efficiency. Therefore, the bond-link element is selected for representing the bond-slip effect in this study.

However, the use of bond-link element in the finite element analysis of RC structures imposes the following restrictions: (1) the finite element mesh must be arranged in the way that a reinforcing bar is located along the edge of a concrete element and (2) a double node is required to represent the relative slip between reinforcing steel and concrete. In a complex structure, particularly in three-dimensional models, these requirements lead to a considerable increase in the number of degrees of freedom, not only because of doubling the number of nodes along the reinforcing steel bars, but also because the mesh has to be refined, so that the bars pass along the edges of concrete elements. The complexity of mesh definition and the large number of degrees of freedom has discouraged researchers from including the bond-slip effect in many previous studies. To address some of these limitations of the bond-link element, a new discrete reinforcing steel model which includes the bond-slip deformation is proposed in this study.

2.2. Material properties

Since the reinforcing steel is used in the concrete construction in the form of reinforcing bars or wire, it is not necessary to introduce the complexities of three-dimensional constitutive relations for steel. Merely the specification of an uniaxial stress-strain relation for steel is sufficient to define the material properties needed in the analysis of reinforced concrete structures. Thus the reinforcing steel is modeled with discrete one-dimensional truss elements, which are assumed to be pin connected and possess one degree of freedom at each node in two dimensional problems. In simulation of material property through the loading history, the reinforcing steel is modeled as a linear elastic, linear strain hardening material with yield stress σ_y as shown in Fig. 2. The reasons for this approximation are: (1) the computational convenience of the model; (2) the behavior of RC members is greatly affected by the yielding of reinforcing steel when the structure is subjected to a large deformation. It is, therefore, advisable to take advantage of the strain-hardening behavior of steel in improving the numerical stability of the solution.

The bond stress is determined from the change in steel stress over a certain measurement length, which is usually taken equal to five bar diameters, and the relative slip is determined

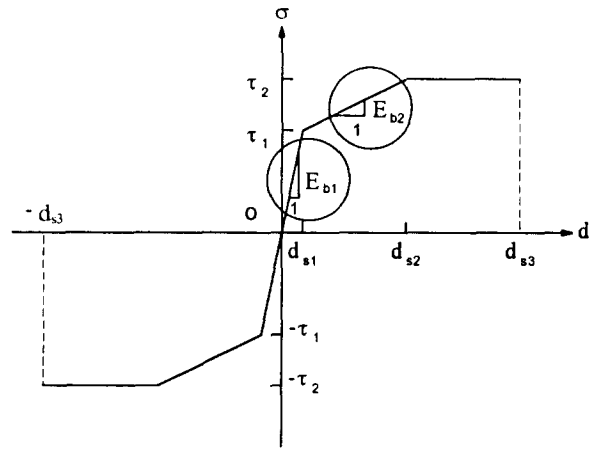

Fig. 3 Bond stress-slip.

externally or internally. It is, therefore, practically impossible to establish a local bond stress-slip relation, since the measured bond stress-slip relation generally represents the average relation over the measurement length. Moreover, the result is very sensitive to the experimental error because the bond stress is derived from the change in steel stress, and the bond-slip relation also depends on the position of the bars, the surface conditions of bars, the loading stage, the boundary conditions and the anchorage length of bars. In spite of these difficulties, several experimental bond-stress slip relations have been proposed (Eligehausen, *et al.* 1983, Hayashi and Kokushō 1985). There are also many simple relations among the proposed models due to these difficulties (ASCE 1982). In this study the simple trilinear bond stress-slip model in Fig. 3 is adopted in the finite element analysis of plane stress problems. The parameters of the model are derived from the material properties of each specimen in the experimental studies. This model is a good approximation of the actual behavior in cases which do not exhibit significant bond-slip and associated bond damage. Under monotonic loading this holds true in all RC members which do not experience anchorage failure.

2.3. Proposed steel model

Based on the aforementioned material models, a new discrete reinforcing steel model which includes the bond-slip deformation is proposed in this study. In this model the reinforcing bar is assumed to be embedded inside the concrete element, as shown in Fig. 4a, so that the analyst can choose the finite element mesh configuration independently of the location of the reinforcing bars(Fig. 5). At the same time the relative slip between reinforcing steel and concrete is explicitly taken into account in the model. Since the finite element model includes the concrete displacement degrees of freedom only, the degrees of freedom which are associated with the reinforcing steel need to be condensed out before the element stiffness matrix of reinforcing bar is assembled into the structure stiffness matrix.

A convenient free body diagram can be drawn which isolates the steel element with the bond-link elements attached at its two end points. Fig. 4b shows the element before deformation and Fig. 4c after deformation. In Fig. 4, i and j denote the end points of the element, points 1 and 3 are associated with concrete and points 2 and 4 are associated with the reinforcing

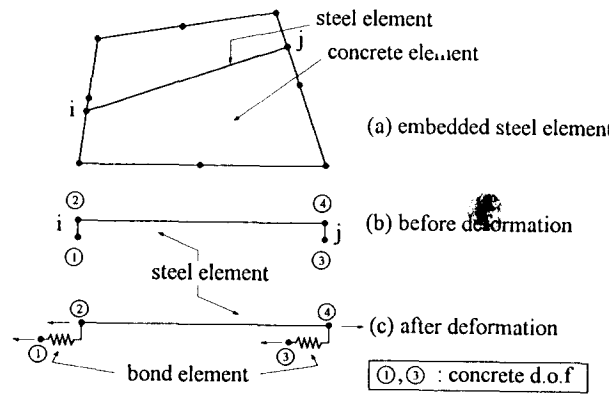

Fig. 4 Discrete reinforcing steel element with bond-slip.

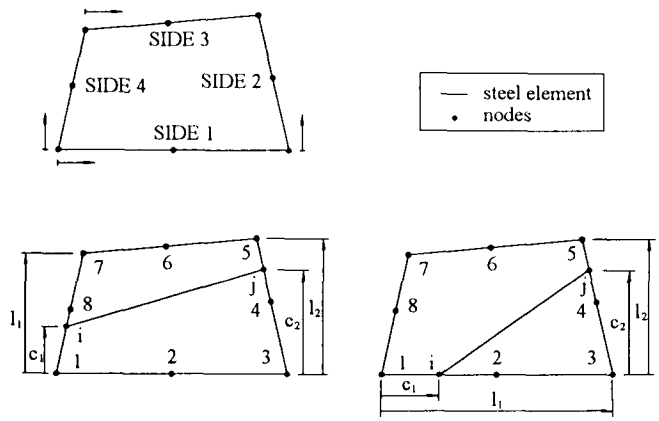

Fig. 5 Steel element embedded in concrete element.

steel at ends i and j, respectively. The corresponding degrees of freedom of the reinforcing steel and concrete at each end are connected by the bond-link element whose stiffness depends on the relative displacement between steel and concrete. With this assumption the stiffness matrix which relates the end displacements along the axis of the reinforcing bar with the corresponding forces can be expressed as follows:

$$\begin{Bmatrix} P_1 \\ P_3 \\ P_2 \\ P_4 \end{Bmatrix} = \begin{bmatrix} k_{bi} & 0 & -k_{bi} & 0 \\ 0 & k_{bj} & 0 & -k_{bj} \\ -k_{bi} & 0 & k_s+k_{bi} & -k_s \\ 0 & -k_{bj} & -k_s & k_s+k_{bj} \end{bmatrix} \cdot \begin{Bmatrix} d_1 \\ d_3 \\ d_2 \\ d_4 \end{Bmatrix} \tag{1}$$

or

$$\begin{Bmatrix} \boldsymbol{P}_c \\ \boldsymbol{P}_s \end{Bmatrix} = \begin{bmatrix} \boldsymbol{K}_{cc} & \boldsymbol{K}_{cs} \\ \boldsymbol{K}_{cs} & \boldsymbol{K}_{ss} \end{bmatrix} \cdot \begin{bmatrix} \boldsymbol{d}_c \\ \boldsymbol{d}_s \end{bmatrix} \tag{2}$$

where $k_s=AE/L$ is the steel stiffness, $k_b=E_bA=E_bm\pi d_bL/2b$ is the stiffness of the bond-link parallel to the bar axis at the corresponding end of the steel element where the dowel action

is neglected, E_b is the slip modulus, A is the bar circumferential area tributary to one bond link element, m is the number of bars of diameter, d_b is the diameter of reinforcing bar, L is the spacing of the bond links along the reinforcing bar, and b is the width of the member cross section. The factor 2 appears in the denominator to account for the fact that it is usually convenient to place bond-link element at both the top and bottom of the reinforcing bar element (ASCE 1982).

By the condensation of the steel degrees of freedom in Eq. (2) the following relation between concrete displacements and corresponding forces results in

$$\{P_c^*\}=[K_{cc}^*]\cdot\{d_c\} \tag{3}$$

where

$$\{P_c^*\}=\{P_c\}-[K_{cs}]\cdot[K_{ss}]^{-1}\cdot\{P_s\} \tag{4}$$

$$[K_{cc}^*]=[K_{cc}]-[K_{cs}]\cdot[K_{ss}]^{-1}\cdot[K_{cs}] \tag{5}$$

After evaluating the inverse of $[K_{ss}]$ and carrying out the multiplications, Eq. (5) is reduced to:

$$[K_{cc}^*]=\frac{k_s\cdot k_{bi}\cdot k_{bj}}{k_s\cdot(k_{bi}+k_{bj})+k_{bi}\cdot k_{bj}}\cdot\begin{bmatrix}1 & -1\\ -1 & 1\end{bmatrix}=[K_{eq}]_s \tag{6}$$

which is the local stiffness matrix of the reinforcing steel element including the effect of bond slip and it is now apparent that bond slip reduces the stiffness of the reinforcing steel element. In case of perfect bond the bond stiffness terms k_{bi} and k_{bj} become infinitely large and the stiffness matrix in Eq. (6) is reduced to the local stiffness of the embedded steel model with perfect bond. The equivalent force vector $\{P^*_c\}$ in Eq. (4) is the nodal forces of steel element including the bond-slip effect and the force is transformed into the concrete degrees of freedom with perfect bond.

Eq. (6) can also be expressed in the global coordinate systems by applying a rotation with angle between the axis of the reinforcing bar and the global x-axis of the structure and has to undergo another transformation before it can be assembled since the end points of the reinforcing steel element do not generally coincide with the nodes of the concrete element mesh. As an example, if the reinforcing bar element crosses the concrete element boundary on sides 2 and 4 in Fig. 5 and the used concrete element has 8 nodes, the transformation matrix $[T]$ which is derived with the procedure used to establish the consistent nodal forces of the finite element method has the following form:

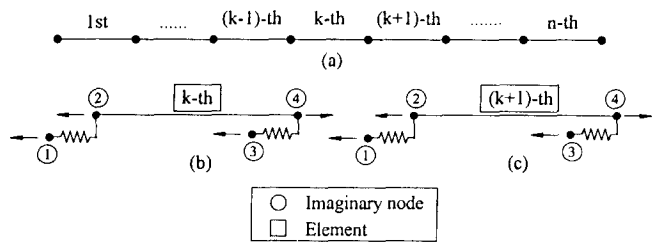

Fig. 6 Modeling of reinforcing bar for matrix method.

$$[T]=\begin{bmatrix} A_1 & 0 & 0 & 0 & 0 & 0 & A_3 & A_2 \\ 0 & 0 & B_1 & B_2 & B_3 & 0 & 0 & 0 \end{bmatrix} \tag{7}$$

where

$$A_1=\begin{bmatrix} 2p^2-3p+1 & 0 \\ 0 & 2p^2-3p+1 \end{bmatrix} \quad A_2=\begin{bmatrix} -4p^2+4p & 0 \\ 0 & -4p^2+4p \end{bmatrix} \quad A_3=\begin{bmatrix} 2p^2-p & 0 \\ 0 & 2p^2-p \end{bmatrix} \tag{8}$$

$$B_1=\begin{bmatrix} 2q^2-3q+1 & 0 \\ 0 & 2q^2-3q+1 \end{bmatrix} \quad B_2=\begin{bmatrix} -4q^2+4q & 0 \\ 0 & -4q^2+4q \end{bmatrix} \quad B_3=\begin{bmatrix} 2q^2-q & 0 \\ 0 & 2q^2-q \end{bmatrix} \tag{9}$$

where $p=c_1/l_1$, $q=c_2/l_2$ and O is the 2×2 null matrix. More details including the case where the steel bar intersects with adjacent two sides of the concrete element can be found elsewhere (Kwak and Filippou 1990).

3. Solution algorithm

Once the displacement increments at the nodes of the concrete finite elements are determined for the current load increment, they can be transformated by the matrix. $[T]$ in Eq. (7) and the rotation matrix to yield the concrete displacement increments $\{\Delta d_c\}$ at the ends of the steel element in the direction of parallel to the axis of the reinforcing bar. Using the second row of Eq. (2) which expresses the condition of equilibrium of the reinforcing bar element, the force and deformation increments in steel can now be determined by assembling the steel element matrices and imposing appropriate boundary conditions at the ends of the entire reinforcing bar.

The solution procedures in this study are basically the same as those of general nonlinear finite element analysis. The newly introduced portion of the algorithm to calculate the steel deformation from the concrete deformation obtained is explained in this section.

If the reinforcing bar is assumed to be subdivided into n elements, as shown in Fig. 6, the relationship for the k-th element can be rearranged as Eq. (10) from Eq. (2).

$$\begin{Bmatrix} \Delta P_2 \\ \Delta P_4 \end{Bmatrix}^k=\begin{bmatrix} k_s+k_{bi} & -k_s \\ -k_s & k_s+k_{bj} \end{bmatrix}^k \cdot \begin{Bmatrix} \Delta d_2 \\ \Delta d_4 \end{Bmatrix}^k - \begin{Bmatrix} k_{bi}\cdot\Delta d_1 \\ k_{bj}\cdot\Delta d_3 \end{Bmatrix} \tag{10}$$

where it should be noted that the concrete displacement increments Δd_1 and Δd_3 are known from the global nonlinear finite element analysis of reinforced concrete structures. Solving Eq. (10) for the force and displacement increment at node 4 yields

$$\begin{Bmatrix} \Delta P_4 \\ \Delta d_4 \end{Bmatrix}^k=[Q]^k \cdot \begin{Bmatrix} \Delta P_2 \\ \Delta d_2 \end{Bmatrix}^k - [R]^k \cdot \begin{Bmatrix} \Delta d_1 \\ \Delta d_3 \end{Bmatrix}^k \tag{11}$$

where

$$[Q]^k=\frac{1}{k_s}\begin{bmatrix} -(k_s+k_{bj}) & k_s\cdot(k_{bi}+k_{bj})+k_{bi}\cdot k_{bj} \\ -1 & k_s+k_{bi} \end{bmatrix}^k \tag{12}$$

$$[R]^k=\begin{bmatrix} k_{bi}\cdot\dfrac{k_s+k_{bj}}{k_s} & k_{bj} \\ \dfrac{k_{bi}}{k_s} & 0 \end{bmatrix}^k \tag{13}$$

For the transition from the k-th to the $(k+1)$-th element using the force equilibrium and the

compatibility condition, Eq. (14) can be obtained

$$\begin{Bmatrix} \Delta P_2 \\ \Delta d_2 \end{Bmatrix}^{k+1} = \begin{Bmatrix} -\Delta P_4 \\ \Delta d_4 \end{Bmatrix}^{k} = \begin{bmatrix} -1 & 0 \\ 0 & 1 \end{bmatrix} \cdot \begin{Bmatrix} \Delta P_4 \\ \Delta d_4 \end{Bmatrix}^{k} = [S] \cdot \begin{Bmatrix} \Delta P_4 \\ \Delta d_4 \end{Bmatrix}^{k} \tag{14}$$

and the substitution of Eq. (11) into Eq. (14) yields Eq. (15).

$$\begin{Bmatrix} \Delta P_2 \\ \Delta d_2 \end{Bmatrix}^{k+1} = [\bar{Q}]^k \cdot \begin{Bmatrix} \Delta P_2 \\ \Delta d_2 \end{Bmatrix}^{k} - [\bar{R}]^k \cdot \begin{Bmatrix} \Delta d_1 \\ \Delta d_3 \end{Bmatrix}^{k} \tag{15}$$

where $[\bar{Q}]^k = [S][Q]^k$ and $[\bar{R}]^k = [S][R]^k$.

Eq. (15) relates the force and displacement increments at the beginning of steel element $k+1$ with those of steel element k. By applying Eq. (15) successively to elements $k-1$, $k-2$, $\cdots$, 2, 1 and summing up the results, the following transfer matrix relation of Eq. (16) is resulted in. After replacing $k+1$ with n in Eq. (16) and applying Eq. (11) for element n, the following relation between the forces and displacements at the two ends of the reinforcing bar can be obtained.

$$\begin{aligned}
\begin{Bmatrix} \Delta P_2 \\ \Delta d_2 \end{Bmatrix}^{k+1} &= [\bar{Q}]^k \cdot \begin{Bmatrix} \Delta P_2 \\ \Delta d_2 \end{Bmatrix}^{k} - [\bar{R}]^k \cdot \begin{Bmatrix} \Delta d_1 \\ \Delta d_3 \end{Bmatrix}^{k} \\
&= [\bar{Q}]^k \cdot [\bar{Q}]^{k-1} \cdot \begin{Bmatrix} \Delta P_2 \\ \Delta d_2 \end{Bmatrix}^{k-1} - [\bar{Q}]^k \cdot [\bar{R}]^{k-1} \cdot \begin{Bmatrix} \Delta d_1 \\ \Delta d_3 \end{Bmatrix}^{k-1} - [\bar{R}]^k \cdot \begin{Bmatrix} \Delta d_1 \\ \Delta d_3 \end{Bmatrix}^{k} \\
&= [\bar{Q}]^k \cdot [\bar{Q}]^{k-1} \cdots [\bar{Q}]^1 \cdot \begin{Bmatrix} \Delta P_2 \\ \Delta d_2 \end{Bmatrix}^{1} - [\bar{Q}]^k \cdot [\bar{Q}]^{k-1} \cdots [\bar{Q}]^2 \cdot [\bar{R}]^1 \cdot \begin{Bmatrix} \Delta d_1 \\ \Delta d_3 \end{Bmatrix}^{1} \\
&\quad - \cdots - [\bar{R}]^k \cdot \begin{Bmatrix} \Delta d_1 \\ \Delta d_3 \end{Bmatrix}^{k}
\end{aligned} \tag{16}$$

$$\begin{aligned}
\begin{Bmatrix} \Delta P_4 \\ \Delta d_4 \end{Bmatrix}^{n} &= [Q]^n \cdot [\bar{Q}]^{n-1} \cdots [\bar{Q}]^1 \cdot \begin{Bmatrix} \Delta P_2 \\ \Delta d_2 \end{Bmatrix}^{1} - [Q]^n \cdot [\bar{Q}]^{n-1} \cdots [\bar{Q}]^2 \cdot [\bar{R}]^1 \cdot \begin{Bmatrix} \Delta d_1 \\ \Delta d_3 \end{Bmatrix}^{1} \\
&\quad - \cdots - [\bar{R}]^n \cdot \begin{Bmatrix} \Delta d_1 \\ \Delta d_3 \end{Bmatrix}^{n}
\end{aligned} \tag{17}$$

As the concrete displacement increments and two boundary conditions are already known at each end of the reinforcing bar element, it is possible now to solve Eq. (17) for the remaining two unknowns among four components of the forces and displacements, namely, ΔP_4^n, Δd_4^n, ΔP_2^1 and Δd_2^1. After obtaining the force and displacement increments at one end of the reinforcing bar, the displacement and the stress of a reinforcing bar including bond-slip at each node can be found through the successive application of Eqs. (11) and (12) which express the condition of equilibrium of the reinforcing bar.

The state determination of the steel and bond elements can now be undertaken yielding the new steel and bond forces and the updated stiffness matrices. The latter are needed only at the beginning of a new load step, when the stiffness matrix of the structure is updated. The substitution of the new steel and bond forces into Eq. (4) yields the equivalent nodal forces at the global degrees of freedom. These forces are subtracted from the applied load increments to yield the unbalanced forces. The process continues until the convergence criterion is satisfied (Fig. 7).

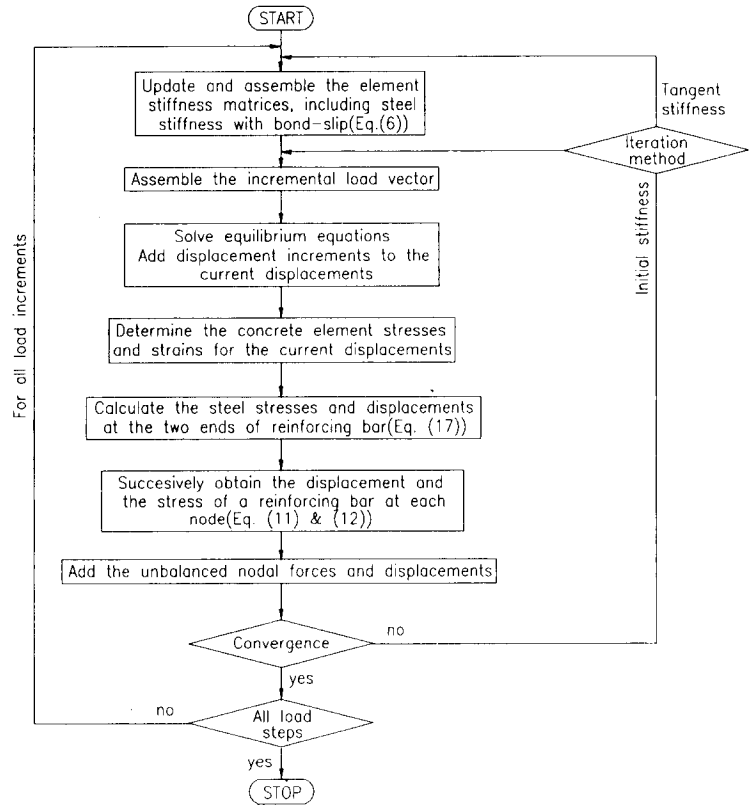

Fig. 7 General solution procedure.

4. Numerical examples

In order to test the proposed reinforcing steel model with bond-slip, the response of anchored reinforcing bars under monotonic pull-out and push-pull loads is studied. Two anchored reinforcing bars tested by Viwathanatepa, Popov and Bertero (1979) to simulate anchorage and loading conditions in the interior beam-column joints of moment resisting frames are selected for the comparison with the proposed reinforcing steel model with bond-slip. The first specimen is an anchored # 8 bar in a well confined block of 25 in.(63.5 cm) width, which corresponds to an anchorage length of 25 bar diameters. This specimen was subjected to a monotonic pull-out under displacement control at one end only. The second specimen also involves a # 8 reinforcing bar with identical dimensions which was subjected to a push-pull loading with gradually increasing end slip value. Both specimens have been the subject of earlier analytical correlation studies by Viwathanatepa, *et al.* (1979), Ciampi, *et al.* (1982), Yankelevky (1985) and Filippou (1986). The material properties of concrete and reinforcing steel are as fellows: the concrete cylinder strength is 4,700 psi (330.5 kg/cm^2) for the specimen under monotonic pull-out and 4,740 psi (333.3 kg/cm^2) for the specimen under push-pull. The yield strength of the reinforcing steel is 68 ksi (4780 kg/cm^2), the yield strain is 0.23% and the modulus of elasticity after yielding is assumed as 411 ksi (28,900 kg/cm^2). Also the parameters used in the bond

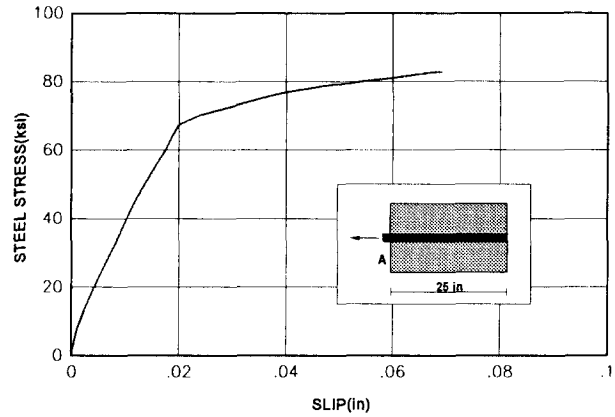

Fig. 8 Stress-slip response of reinforcing bar at point A (1 in=2.54 cm, 1 ksi=70.31 kg/cm^2).

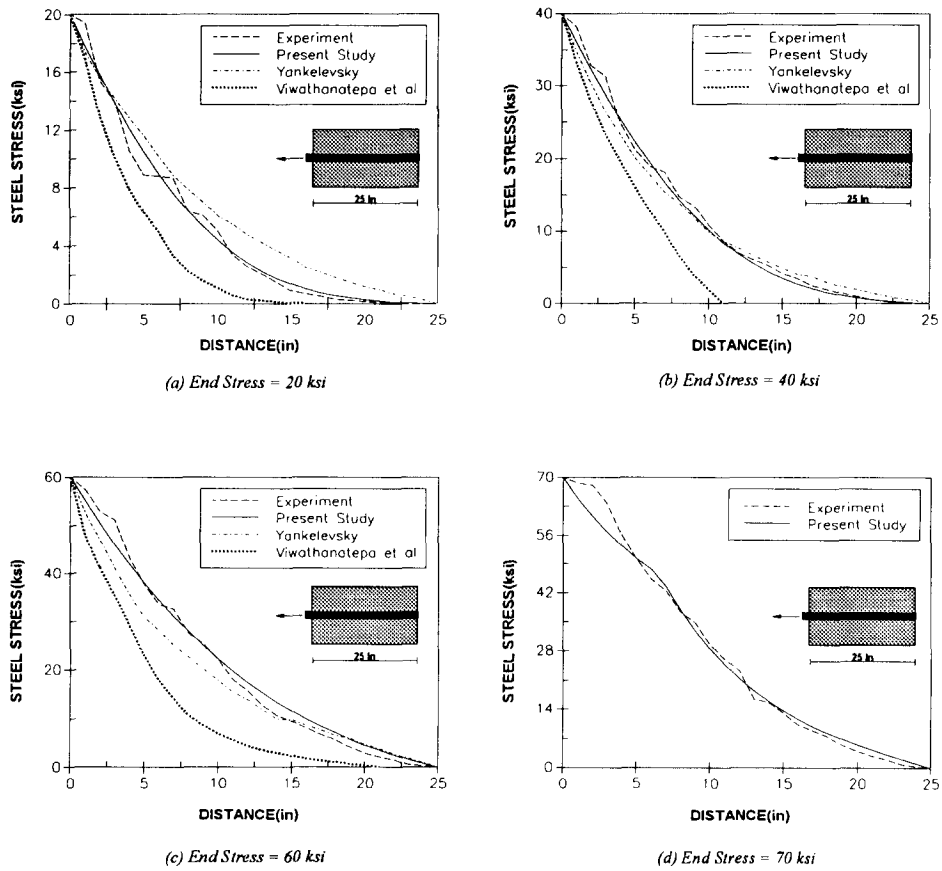

(a) End Stress = 20 ksi

(b) End Stress = 40 ksi

(c) End Stress = 60 ksi

(d) End Stress = 70 ksi

Fig. 9 Stress distribution along anchored reinforcing bar under pull-out loading (1 in=2.54 cm, 1 ksi=70.31 kg/cm^2)

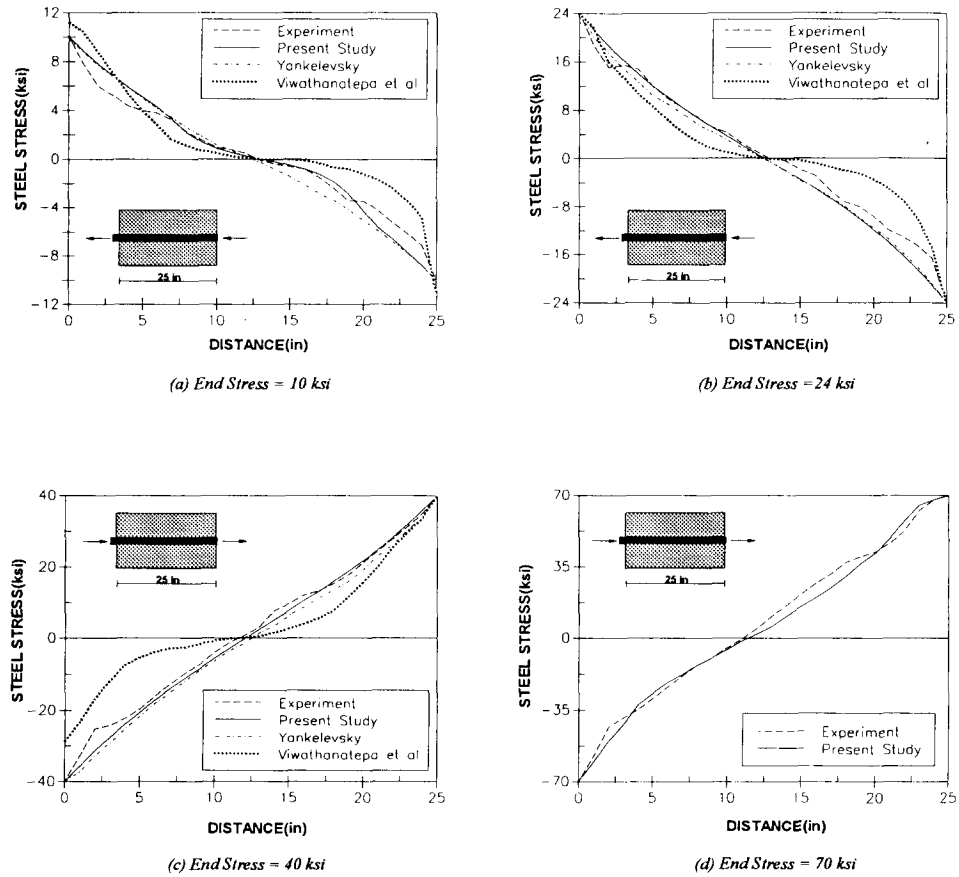

Fig. 10 Stress distribution along anchored reinforcing bar under push-pull loading (1 in=2.54 cm, 1 ksi=70.31 kg/cm^2)

model are equal to those used by Filippou, *et al.* (1983) and Filippou (1986) in earlier investigations, namely: $u_1=0.02756$ in (0.07 cm), $u_2=0.07874$ in (0.2 cm), $u_3=0.2756$ in (0.7 cm), $\tau_1=1500$ psi (105.5 kg/cm^2) and $\tau_2=2350$ psi (165.2 kg/cm^2) (Fig. 3). In the study by Ciampi, *et al.* (1982) the bond-slip relation was modified in the outer unconfined portions along the entire anchorage length. For the sake of simplicity in the present study, the same bond stress-slip relation is used along the entire anchorage length. Under push-pull loading conditions, this assumption leads to underestimation of the bond resistance at the push-in end of the reinforcing bar. Twenty-five(25) steel elements of 1 inch length were used in modeling the anchored reinforcing bar.

Fig. 8 shows the analytical relation between pull-out slip and steel stress at one end of the reinforcing bar under monotonic pull-out loading. Figs. 9a-9d show the distribution of steel stresses along the anchorage length of the reinforcing bar at different loading stages. The experimental results are compared with the analytical results of Viwathanatepa, *et al.* (1979), Yankelevsky (1985) and those of the present study. The result of the present study show the best agreement, particularly, with increasing load. It should be noted that the model of Yankelevsky does not allow for yielding of the reinforcing steel. The results by Viwathanatepa, *et al.* are from a linear finite element analysis, since no stress distributions are presented for the nonlinear model proposed

in that study.

The examples of steel stress distributions along the anchorage length of the reinforcing bar under push-pull loading are shown in Figs. 10a-10d. The results of the proposed model show an excellent agreement with experimental results. However, the comparison of the overall response shows small discrepancies between the present model and the experimental data. Two factors are attributable to this: (1) the present model is tested under load controlled conditions, while the experimental specimen was subjected to displacement controlled testing, and (2) the assumption that the bond stress-slip relation is the same along the anchorage length of the bar is not adequate for the large deformation stage where a significant bond damage can occur. However, it is observed that the proposed reinforcing steel model with bond-slip can describe quite well the response of anchored reinforcing bars under monotonic pull-out and push-pull loading conditions.

5. Conclusions

A new reinforcing steel model which is embedded inside a concrete element and accounts for the effect of bond-slip is developed. Unlike the classical bond-link and bond-zone element which have the restrictions in the numerical modeling such as a reinforcing bar arrangement along the edge of a concrete element and a double node to represent the relative slip between reinforcing steel and concrete, the proposed model which does not take the double nodes can yield significant savings in the number of nodes needed to account for the effect of bond-slip, particularly, in three dimensional finite element models. A new nonlinear solution scheme based on the equilibrium at each node of steel and the compatibility condition between steel and concrete is developed in connection with this model. The efficiency and reliability of the proposed model are demonstrated through the correlation studies between analytical and experimental results and the parametric studies associated with them.

References

ASCE Task Committee on Finite Element Analysis of Reinforced Concrete Structures (1982), *State-of-the-Art Report on Finite Element Analysis of Reinforced Concrete,* ASCE Special Publications.

Choi, C. K. and Kwak, H. G. (1990), "The effect of finite element mesh sizes in nonlinear finite element analysis of R/C structures," *Computers and Structures,* **36**(4), 175-186.

Ciampi, V., Eligehausen, R., Popov, E. P. and Bertero, V. V. (1982), "Analytical model for concrete anchorages of reinforcing bars under generalized excitations," *Report No. UCB/EERC-82/23,* Earthquake Engineering Research Center, University of California, Berkeley.

de Groot, A. K., Kusters, G. M. A. and Monnier, T. (1981), "Numerical modeling of bond-slip behavior," *Heron, Concrete Mechanics,* **26**(1B).

Eligehausen, R., Popov, E. P. and Bertero, V. V. (1983), "Local bond stress-slip relationships of deformed bars under generalized excitations," *Report No. UCB /EERC 83-23,* Earthquake Engineering Research Center, University of California, Berkeley.

Filippou, F. C. (1986), "A simple model for reinforcing bar anchorages under cyclic excitations," *Journal of Structural Engineering, ASCE,* **112**(7), 1639-1659.

Filippou, F. C., Popov, E. P. and Bertero, V. V. (1983), "Effects of bond deterioration on hysteretic behavior of reinforced concrete joints," *Report No. UCB/EERC-83/19,* Earthquake Engineering Research Center, University of California, Berkeley.

Hayashi, S. and Kokusho, S. (1985), "Bond behavior in the neighborhood of the crack," *Proceedings*

of the U.S.-Japan Joint Seminar on Finite Element Analysis of Reinforced Concrete, Tokyo, Japan, 364-373.

Keuser, M. and Mehlhorn, G. (1987), "Finite element models for bond problems," *Journal of Structural Engineering, ASCE,* **113**(10), 2160-2173.

Kwak, H. G. and Filippou, F. C. (1990), "Finite element analysis of reinforced concrete structures under monotonic loads," *Report No. UCB/SEMM-90/14,* University of California, Berkeley.

Leibengood, L. D., Darwin, D. and Dodds, R. H. (1986), "Parameters affecting FE analysis of concrete structures," *Journal of Structural Engineering, ASCE,* **112**(2), 326-341.

Ngo, D. and Scordelis, A. C. (1967), "Finite element analysis of reinforced concrete beams," *Journal of ACI,* **64**(3), 152-163.

Viwathanatepa, S., Popov, E. P. and Bertero, V. V. (1979), "Seismic behavior of reinforced concrete interior beam-column subassemblages," *Report No. UCB/EERC-79/14,* Earthquake Engineering Research Center, University of California, Berkeley.

Yankelevsky, D. Z. (1985), "New finite element for bond-slip analysis," *Journal of Structural Engineering, ASCE,* **111**(7), 1533-1542.